

# Modelling Point Referenced Spatial Count Data: A Poisson Process Approach

Diego Morales-Navarrete<sup>1</sup>, Moreno Bevilacqua<sup>2</sup>, Christian  
Caamaño-Carrillo<sup>3</sup>, and Luis M. Castro<sup>4</sup>

<sup>1,4</sup>Departamento de Estadística, Pontificia Universidad Católica de Chile,  
Santiago, Chile

<sup>1,2,4</sup>Millennium Nucleus Center for the Discovery of Structures in Complex  
Data, Chile, `dbmorales@mat.uc.cl`

<sup>2</sup>Facultad de Ingeniería y Ciencias, Universidad Adolfo Ibáñez, Viña del  
Mar, Chile, `moreno.bevilacqua@uai.cl`

<sup>3</sup>Departamento de Estadística, Universidad del Bío-Bío, Concepción, Chile,  
`chcaaman@ubiobio.cl`

<sup>4</sup>Centro de Riesgos y Seguros UC, Pontificia Universidad Católica de Chile,  
Santiago, Chile, `mcastro@mat.uc.cl`

May 11, 2021

## Abstract

Random fields are useful mathematical tools for representing natural phenomena with complex dependence structures in space and/or time. In particular, the Gaussian random field is commonly used due to its attractive properties and mathematical tractability. However, this assumption seems to be restrictive when dealing with counting data. To deal with this situation, we propose a random field with a Poisson marginal distribution by considering a sequence of independent copies of a random field with an exponential marginal distribution as 'inter-arrival times' in the counting renewal processes framework. Our proposal can be viewed as a spatial generalization of the Poisson process.

Unlike the classical hierarchical Poisson Log-Gaussian model, our proposal generates a (non)-stationary random field that is mean square continuous and with Poisson marginal distributions. For the proposed Poisson spatial random field, analytic expressions for the covariance function and the bivariate distribution are provided. In an extensive simulation study, we investigate the weighted pairwise likelihood as a method for estimating the Poisson random field parameters.

Finally, the effectiveness of our methodology is illustrated by an analysis of reindeer pellet-group survey data, where a zero-inflated version of the proposed model is compared with zero-inflated Poisson Log-Gaussian and Poisson Gaussian copula models. Supplementary materials for this article, include technical proofs and R code for reproducing the work, are available as an online supplement.

Keywords: Gaussian random field; Gaussian copula; Pairwise likelihood function; Poisson distribution; Renewal process

## 1. INTRODUCTION

The faecal pellet count technique is one of the most popular tools for estimating an animal species' abundance. Specifically, this technique uses the number of observed droppings combined with their decay time and the target animal species' defecation rate. With these ingredients, it is possible to obtain an accurate density estimation of an animal population. This method was proposed by [Bennett et al. \(1940\)](#) and has been improved by several au-

thors since then (see for instance [Etten and Bennett, 1965](#); [Mayle et al., 1999](#); [Krebs et al., 2001](#), among others).

The study motivating our research is a reindeer pellet-group survey conducted in the northern forest area of Sweden and previously analysed by [Lee et al. \(2016\)](#). The goal of this survey was to assess the impact of newly established wind farms on reindeer habitat selection. This choice is crucial for the reindeer since it involves trade-offs between fulfilling necessities for feeding, mating, parental care, and risk mitigation of predation ([Sivertsen et al., 2016](#)).

Survey data were collected over the years 2009–2010 and present a large number of zero counts. This situation frequently occurs when spatial species count data are collected because the survey is conducted using a point transect design ([Buckland et al., 2001](#)). This design considers a set of  $K$  points as systematically spaced points along lines located throughout the survey region, where  $k$  should be at least 20 for obtaining robust estimates of the abundance. In our case, the study area was 250 km<sup>2</sup>, which is the distance between each transect of 300 m. On each transect, the distance between each plot 100 m. [Figure 1](#), taken from [Buckland et al. \(2001\)](#), presents two examples of point transect surveys in which the points are systematically spaced along lines.

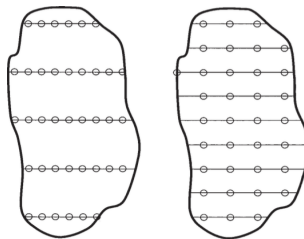


Figure 1: Examples of point transect survey design

From a modelling viewpoint, the analysis of the reindeer pellet-group data requires the development of statistical models for geo-referenced count data that take into account both the spatial dependence and the excessive number of zeros. Random fields or stochastic processes are useful models when dealing with geo-referenced spatial or spatio-temporal data ([Stein, 1999](#); [Cressie and Wikle, 2011](#); [Banerjee et al., 2014](#)). In particular, the Gaussian random field is widely used due to its attractive properties and mathematical tractability

(Gelfand and Schliep, 2016). Gaussianity is clearly a restrictive assumption when dealing with counting data. However, many models of current use for spatial count data employ Gaussian random fields as building blocks.

The first example is the hierarchical model approach proposed by Diggle et al. (1998), which can be viewed as a generalized linear mixed model (Diggle and Ribeiro, 2007; Diggle and Giorgi, 2019). Under this framework, non-Gaussian models for spatial data can be specified using a link function and a latent Gaussian random field through a conditionally independent assumption. In particular, the Poisson Log-Gaussian random field (Poisson LG hereafter) has been widely applied for modelling count spatial data (see for instance Christensen and Waagepetersen, 2002; Guillot et al., 2009; De Oliveira, 2013, for interesting applications and in-depth study of its properties). Similar models, that can be defined hierarchically in terms of the specification of the first two moments and a correlation function have been proposed in Monestiez et al. (2006) and De Oliveira (2014).

It is important to stress that the conditional independence assumption underlying these kind of models leads to (a) random fields with marginal distributions that are not Poisson and (b) random fields with a “forced” nugget effects that implies no mean square continuity.

To illustrate this situation, Figure 2 (a) shows a realization on the unit square of a Poisson LG random field, assuming  $e^{\mu + \sqrt{\sigma^2}G(\mathbf{s})}$  as an LG random field, where  $G$  is the standard Gaussian random field with isotropic correlation  $\rho(r) = (1 - r/0.5)_+^4$  belonging to the Generalized Wendland family (Bevilacqua et al., 2019),  $\mu = 0.5$ ,  $\sigma^2 = 0.05$ ,  $r$  is the spatial distance and  $(\cdot)_+$  denotes the positive part. In this case, the mean of the Poisson LG field is given by  $\lambda = e^{0.5 + 0.05/2}$ . The associated histogram is shown in panel (d).

Additionally, Figure 2 (b) shows a realization and the associated histogram of our proposed random field (see Equation (2)), with the same mean and underlying correlation function of the Poisson LG model. A quick analysis of both figures reveal a “whitening” effect on the Poisson LG random field’s paths because of the “forced” discontinuity at the origin of the correlation function of the Poisson LG (see Section 3.1). This potential problem, which has also been highlighted by De Oliveira (2013), indicates that the Poisson LG random field may impose severe restrictions on the correlation structure and may be inadequate to model

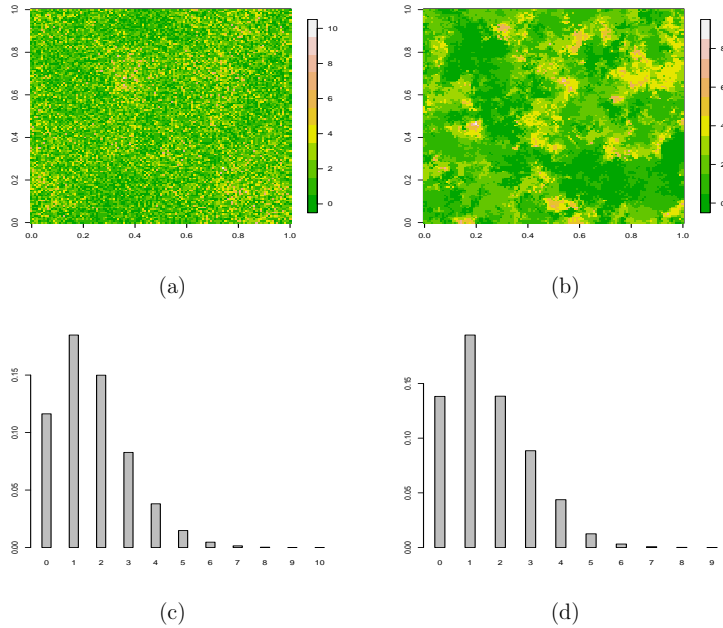


Figure 2: A realization of a Poisson LG random field, where the LG random field is given by  $e^{\mu + \sqrt{\sigma^2}G(\mathbf{s})}$ , where  $G$  is a standard Gaussian random field with parameters  $\mu = 0.5$  and  $\sigma^2 = 0.05$  (panel a) and its associated histogram (panel c). A realization of our proposed Poisson random field with  $\lambda = e^{0.5 + 0.05/2}$  (panel b) and its associated histogram (panel d). In both cases the underlying isotropic correlation is  $\rho(r) = (1 - r/0.5)_+^4$ .

spatial count data mostly consisting of small counts.

The second example is the Poisson spatial model obtained using Gaussian copula ([Kaziánka and Pilz, 2010](#); [Masarotto and Varin, 2012](#); [Joe, 2014](#)), which is referred to as the Poisson GC random field hereafter. This approach has some potential benefits with respect to the hierarchical models (see [Han and De Oliveira, 2016](#), for a comparison between these two approaches). For instance, the resulting random field has Poisson marginals and can be mean square continuous or not depending on if the latent Gaussian random field is mean square continuous or not. In addition to some criticisms concerning the lack of uniqueness of the copula when applied to discrete data ([Genest and Nešlehová, 2007](#); [Trivedi and Zimmer, 2017](#)), in this approach it is not clear what the underlying physical mechanism generating the data is, making it less interesting from an interpretability perspective.

Our proposal tries to solve the drawbacks of the Poisson LG and of the Poisson GC approaches by specifying a new class of spatial counting random fields based on the Poisson counting process ([Cox, 1962](#); [Mainardi et al., 2007](#); [Ross, 2008](#)) applied to the spatial setting.

Specifically, we first consider a random field with exponential marginal distributions obtained as a rescaled sum of two independent copies of an underlying standard Gaussian random field. Then, by considering independent copies of the exponential random field as 'inter-arrival times' in the counting renewal processes framework, we obtain a (non-)stationary random field with Poisson marginal distributions. As a consequence, the proposed model can be viewed as a spatial generalization of the Poisson process.

For the novel Poisson random field, we provide the covariance function and analytic expressions for the bivariate distribution in terms of the regularized incomplete Gamma and confluent hypergeometric functions ([Gradshteyn and Ryzhik, 2007](#)). It turns out that the dependence of the proposed Poisson random field is indexed by the correlation function of the underlying Gaussian random field and by the mean parameter. It is important to stress that our theoretical results are inspired by the two-dimensional renewal theory described in [Hunter \(1974\)](#).

The Poisson random field estimation is conducted using the weighted pairwise likelihood (*wpl*) method ([Lindsay, 1988](#); [Varin et al., 2011](#); [Bevilacqua and Gaetan, 2015](#)) to exploit the results obtained about the bivariate distribution. In particular, in an extensive simulation study, we explore the efficiency of the *wpl* method when estimating the parameters of the proposed Poisson random field. We also explore the statistical efficiency of a Gaussian misspecified version of the *wpl* method ([Gouriéroux et al., 2017](#); [Bevilacqua et al., 2021](#)), which is also called Gaussian quasi-likelihood in some literature ([Masuda, 2013](#)). The findings show that the misspecified *wpl* leads to a less efficient estimator, in particular for low counts. However, the method has some computational benefits. In addition, we compare the performance of the optimal linear predictor under the proposed model with the optimal predictors obtained using the Poisson GC and Poisson LG models.

Finally, in the real data application, we consider a zero-inflated version of the proposed Poisson random field to deal with excess zeros in the reindeer pellet-group counts data using the zero-inflated Poisson LG and Poisson GC models as benchmarks. The methods proposed in this paper are implemented in the R ([R Core Team, 2020](#)) package `GeoModels` ([Bevilacqua et al., 2019](#)) and R code for reproducing the work is available as an online

supplement.

The remainder of the paper is organized as follows. In Section 2, we provide some basic notation and describe the exponential random field. Section 3 introduces our proposal by presenting a new class of counting random fields under the general renewal counting framework, focusing on the Poisson random field. A study of the correlation function and bivariate distribution is also presented. In Section 4, the *wpl* method for obtaining the *wpl* estimates and the optimal linear prediction are discussed. Section 5 provides an in-depth simulation study to investigate the performance of the Poisson random field in spatial and spatio-temporal settings. In Section 6, the faecal pellet-group counts dataset previously described is re-analysed. Section 7 closes the paper with a discussion of our main findings and future research directions.

## 2. A RANDOM FIELD WITH EXPONENTIAL MARGINAL DISTRIBUTIONS

To make the paper self-contained, we start by introducing some notation in this Section. For the rest of the paper, given a second order real-valued random field  $Q = \{Q(\mathbf{s}), \mathbf{s} \in A \subset \mathbb{R}^d\}$ , we denote by  $f_{Q(\mathbf{s})}$  and  $F_{Q(\mathbf{s})}$  the marginal probability density function (*pdf*) and cumulative distribution function (*cdf*) of  $Q(\mathbf{s})$ , respectively. Moreover, for any set of distinct points  $(\mathbf{s}_1, \dots, \mathbf{s}_n)^T$ ,  $n \in \mathbb{N}$  and  $\mathbf{s}_i \in A$ , we denote the correlation function by  $\rho_Q(\mathbf{s}_i, \mathbf{s}_j) = \text{Corr}(Q(\mathbf{s}_i), Q(\mathbf{s}_j))$ . In the stationary case, the notation adopted is  $\rho_Q(\mathbf{h}) = \text{Corr}(Q(\mathbf{s}_i), Q(\mathbf{s}_j))$ , where  $\mathbf{h} = \mathbf{s}_i - \mathbf{s}_j$  is the lag separation vector. Finally,  $f_{\mathbf{Q}_{ij}}$  denotes the *pdf* of the bivariate random vector  $\mathbf{Q}_{ij} = (Q(\mathbf{s}_i), Q(\mathbf{s}_j))^T$ ,  $i \neq j$ . If the random field  $Q$  is a discrete-valued random field, then  $\Pr(Q(\mathbf{s}) = l)$  and  $\Pr(Q(\mathbf{s}_i) = n, Q(\mathbf{s}_j) = m)$ ,  $l, m, n \in \mathbb{N}$  will denote the marginal and bivariate discrete probability functions, respectively.

Let  $G = \{G(\mathbf{s}), \mathbf{s} \in A\}$  a zero mean and unit variance weakly stationary Gaussian random field with correlation function  $\rho_G(\mathbf{h})$ . Henceforth, we call  $G$  the Gaussian underlying random field, and with some abuse of notation, we set  $\rho(\mathbf{h}) := \rho_G(\mathbf{h})$ , denoting this as the underlying correlation function. Let  $G_1, G_2$  be two independent copies of  $G$  and let us define the random

field  $W = \{W(\mathbf{s}), \mathbf{s} \in A\}$  as follows:

$$W(\mathbf{s}) := \frac{1}{2\lambda(\mathbf{s})} \sum_{k=1}^2 G_k^2(\mathbf{s}), \quad (1)$$

where  $\lambda(\mathbf{s}) > 0$  is a non-random function.  $W$  is a stationary random field with a marginal exponential distribution, with parameter  $\lambda(\mathbf{s})$  denoted by  $W(\mathbf{s}) \sim \text{Exp}(\lambda(\mathbf{s}))$  with  $\mathbb{E}(W(\mathbf{s})) = 1/\lambda(\mathbf{s})$ ,  $\text{Var}(W(\mathbf{s})) = 1/\lambda^2(\mathbf{s})$ , and it can be easily observed that  $\rho_W(\mathbf{h}) = \rho^2(\mathbf{h})$ .

The associated multivariate exponential density was discussed earlier by [Krishnamoorthy and Parthasarathy \(1951\)](#), and its properties have been studied since then by several authors ([Krishnaiah and Rao, 1961](#); [Royen, 2004](#)). However, likelihood-based methods for exponential random fields can be troublesome since the analytical expressions of the multivariate density can be derived only in some special cases. For example, when  $d = 1$  and the underlying correlation function is exponential the multivariate *pdf* is given by ([Bevilacqua et al., 2020](#)):

$$\begin{aligned} f_W(w_1, \dots, w_n) &= \exp \left[ -\frac{w_1 \lambda_1}{(1 - \rho_{1,2}^2)} - \frac{w_n \lambda_n}{(1 - \rho_{n-1,n}^2)} - \sum_{i=2}^{n-1} \frac{(1 - \rho_{i-1,i}^2 \rho_{i,i+1}^2) \lambda_i w_i}{(1 - \rho_{i-1,i}^2)(1 - \rho_{i,i+1}^2)} \right] \\ &\quad \times \prod_{i=1}^{n-1} I_0 \left( \frac{2\rho_{i,i+1} \sqrt{w_i \lambda_i w_{i+1} \lambda_{i+1}}}{(1 - \rho_{i,i+1}^2)} \right) \times \left( \prod_{i=1}^{n-1} (1 - \rho_{i,i+1}^2) \right)^{-1}, \end{aligned}$$

with  $\rho_{ij} := \exp\{-|s_i - s_j|/\phi\}$ ,  $\lambda_i = \lambda(s_i)$ ,  $\phi > 0$  and  $I_a(x)$  being the modified Bessel function of the first kind of order  $a$ . Regardless of the dimension of the space  $A$  and the type of correlation function, the bivariate exponential *pdf* is given by ([Kibble, 1941](#); [Vere-Jones, 1997](#)):

$$f_{W_{ij}}(w_i, w_j) = \frac{e^{-\frac{(\lambda(\mathbf{s}_i)w_i + \lambda(\mathbf{s}_j)w_j)}{(1 - \rho^2(\mathbf{h}))}}}{(1 - \rho^2(\mathbf{h}))} I_0 \left( \frac{2\sqrt{\rho^2(\mathbf{h})\lambda(\mathbf{s}_i)\lambda(\mathbf{s}_j)w_i w_j}}{(1 - \rho^2(\mathbf{h}))} \right).$$

The exponential random field  $W$  will be used next for defining a new random field with Poisson marginal distributions.

### 3. SPATIAL POISSON RANDOM FIELDS

Our proposal relies on considering an infinite sequence of independent copies  $Y_1, Y_2, \dots$ , of  $Y = \{Y(\mathbf{s}), \mathbf{s} \in A\}$ , a positive continuous random field. First, we define a new class of counting random fields,  $N_t := \{N_t(\mathbf{s}), \mathbf{s} \in A\}$ ,  $t \geq 0$ , as follows:

$$N_t(\mathbf{s}) := \begin{cases} 0 & \text{if } 0 \leq t < S_1(\mathbf{s}) \\ \max_{n \geq 1} \{S_n(\mathbf{s}) \leq t\} & \text{if } S_1(\mathbf{s}) \leq t \end{cases}, \quad (2)$$

where  $S_n(\mathbf{s}) = \sum_{i=1}^n Y_i(\mathbf{s})$  is the  $n$ -fold convolution of  $Y$ . This model can be viewed as a spatial generalization of the renewal counting processes (Cox, 1962; Mainardi et al., 2007), where we consider independent copies of a positive random field as “inter-arrival times” instead of an independent and identically distributed sequence of positive random variables.

For each  $\mathbf{s} \in A$ , and using the classical results from the renewal counting processes theory, the marginal discrete probability function of  $N$  is given by:

$$\Pr(N_t(\mathbf{s}) = n) = F_{S_n(\mathbf{s})}(t) - F_{S_{n+1}(\mathbf{s})}(t). \quad (3)$$

In addition, the marginal mean (the so-called renewal function) and the variance of  $N_t$  are given, respectively, by:

$$\mathbb{E}(N_t(\mathbf{s})) = \sum_{i=1}^{\infty} F_{S_i(\mathbf{s})}(t), \quad \text{Var}(N_t(\mathbf{s})) = \left( 2 \sum_{i=1}^{\infty} i F_{S_i(\mathbf{s})}(t) - \mathbb{E}(N_t(\mathbf{s})) \right) - (\mathbb{E}(N_t(\mathbf{s})))^2.$$

Different elections of the positive random field  $Y$  lead to counting random fields with specific marginal distributions.

In this paper, we assume that  $Y \equiv W$ , where  $W$  is the positive random field defined in (1), with  $\text{Exp}(\lambda(\mathbf{s}))$  marginal distribution and *cdf* given by  $F_{Y(\mathbf{s})}(x) = 1 - e^{-\lambda(\mathbf{s})x}$ ,  $x > 0$ . In this case,  $S_n(\mathbf{s}) \sim \text{Gamma}(n, \lambda(\mathbf{s}))$  with  $n \in \mathbb{N}$  is an Erlang distribution, with *cdf* given by:

$$F_{S_n(\mathbf{s})}(x) = 1 - \sum_{k=0}^{n-1} \frac{e^{-\lambda(\mathbf{s})x} (\lambda(\mathbf{s})x)^k}{k!}, \quad x > 0$$

and from (3), we can obtain the marginal distribution of  $N$  as:

$$\Pr(N_t(\mathbf{s}) = n) = e^{-t\lambda(\mathbf{s})}[t\lambda(\mathbf{s})]^n/n!, \quad n = 0, 1, 2, \dots \quad (4)$$

with  $\mathbb{E}(N_t(\mathbf{s})) = \text{Var}(N_t(\mathbf{s})) = t\lambda(\mathbf{s})$ . Then,  $N_t(\mathbf{s}) \sim \text{Poisson}(t\lambda(\mathbf{s}))$  is the random number of renewals occurring in the temporal interval  $(0, t]$  for each location site  $\mathbf{s}$ . Additionally,  $t\lambda(\mathbf{s})$  is the expected number of arrivals in an interval of length  $t$  for each location site  $\mathbf{s}$ . Hereafter and without loss of generality,  $t$  is set to one, and  $N_t$  is denoted as  $N$ . We will call  $N$  a Poisson random field with underlying correlation  $\rho(\mathbf{h})$  because  $N$  is marginally Poisson distributed and the dependence is indexed by a correlation function.

Note that, when the spatially varying mean (and variance)  $\lambda(\mathbf{s})$  is not constant then  $N$  is not stationary. A typical parametric specification for the mean is given by  $\lambda(\mathbf{s}) = e^{X(\mathbf{s})^T\boldsymbol{\beta}}$ , where  $X(\mathbf{s}) \in \mathbb{R}^k$  is a vector of covariates and  $\boldsymbol{\beta} \in \mathbb{R}^k$  even though other types of parametric and non-parametric specifications can be used.

It is important to note that although the proposed Poisson random field is defined on the  $d$ -dimensional Euclidean space  $A$ , the proposed method can be easily adapted to other spaces, such as the space-time space or the spherical spaces. The key for this extension is the specification of a suitable underlying correlation function  $\rho(\mathbf{h})$ . For instance, a correlation function defined on the space-time setting, *i.e.*,  $A \subset \mathbb{R}^d \times \mathbb{R}$  (Gneiting, 2002) or on the sphere of arbitrary radius *i.e.*,  $A \subseteq \mathbb{S}^2 = \{\mathbf{s} \in \mathbb{R}^3, \|\mathbf{s}\| = M\}$ ,  $M > 0$  (Gneiting, 2013; Porcu et al., 2016). In the case of lattice or areal data, a suitable precision matrix with an appropriate neighbourhood structure should be specified for the underlying Gaussian Markov random field (Rue and Held, 2005).

### 3.1 Correlation function

The following result, which can be obtained from the pioneering work of Hunter (1974), provides the correlation function  $\rho_N(\mathbf{s}_i, \mathbf{s}_j)$  of the non-stationary Poisson random field with underlying correlation  $\rho(\mathbf{h})$  depending on the regularized lower incomplete gamma function:

$$\gamma^*(a, x) = \frac{\gamma(a, x)}{\Gamma(a)} = \frac{1}{\Gamma(a)} \int_0^x t^{a-1} e^{-t} dt, \quad (5)$$

where  $\gamma(\cdot, \cdot)$  is the lower incomplete gamma function and  $\Gamma(\cdot)$  is the Gamma function. Additionally, we define the function  $\gamma^*(a, x, x') = \gamma^*(a, x) \gamma^*(a, x')$ , which considers the product of two regularized lower incomplete gamma function sharing a common parameter.

**Theorem 1.** *Let  $N$  be a non-stationary Poisson random field with underlying correlation  $\rho(\mathbf{h})$ . Then,*

$$\rho_N(\mathbf{s}_i, \mathbf{s}_j) = \frac{\rho^2(\mathbf{h})(1 - \rho^2(\mathbf{h}))}{\sqrt{\lambda(\mathbf{s}_i)\lambda(\mathbf{s}_j)}} \sum_{r=0}^{\infty} \gamma^* \left( r + 1, \frac{\lambda(\mathbf{s}_i)}{1 - \rho^2(\mathbf{h})}, \frac{\lambda(\mathbf{s}_j)}{1 - \rho^2(\mathbf{h})} \right),$$

with  $\mathbf{h} = \mathbf{s}_i - \mathbf{s}_j$ .

**Proof.** See [Hunter \(1974\)](#).

**Corollary 1.** *In Theorem 1, when  $\lambda(\mathbf{s}) = \lambda$ , the Poisson random field is weakly stationary with the correlation function given by:*

$$\rho_N(\mathbf{h}, \lambda) = \rho^2(\mathbf{h}) [1 - \exp(-z(\mathbf{h}, \lambda)) (I_0(z(\mathbf{h}, \lambda)) + I_1(z(\mathbf{h}, \lambda)))], \quad (6)$$

where  $z(\mathbf{h}, \lambda) = 2\lambda(1 - \rho^2(\mathbf{h}))^{-1}$ .

**Proof.** See the online supplement.

Note that  $\rho_N(\mathbf{h})$  is well defined at the origin since  $\rho_N(\mathbf{h}) = 1$ , as  $\mathbf{h} \rightarrow \mathbf{0}$ , implying that the Poisson random field is weakly stationary and mean square continuous. Additionally, if  $\rho(\mathbf{h}) = 0$ , then  $\rho_N(\mathbf{h}) = 0$  and if  $\lambda \rightarrow \infty$  then  $\rho_N(\mathbf{h}) = \rho^2(\mathbf{h})$ , *i.e.*, it converges to the correlation function of an exponential random field.

Following the graphical example given in [Figure 2](#), we now compare the correlation functions of the proposed Poisson random field with the correlation of the Poisson LG random field, which is defined hierarchically by first considering a LG random field  $Z = \{Z(\mathbf{s}), \mathbf{s} \in A\}$  defined as  $Z(\mathbf{s}) = e^{\mu + \sigma^2 G(\mathbf{s})}$ , where  $G$  is a standard Gaussian random field with correlation  $\rho(\mathbf{h})$ , and then assuming  $Y(\mathbf{s}) | Z(\mathbf{s}) \sim \text{Poisson}(Z(\mathbf{s}))$  with  $Y(\mathbf{s}_i) \perp\!\!\!\perp Y(\mathbf{s}_j) | Z$  for  $i \neq j$ . In this case, the first two moments of  $Y(\mathbf{s})$  are given by  $\mathbb{E}(Y(\mathbf{s})) = e^{\mu + 0.5\sigma^2}$  and  $\text{Var}(Y(\mathbf{s})) = \mathbb{E}(Y(\mathbf{s}))(1 + \mathbb{E}(Y(\mathbf{s}))(e^{\sigma^2} - 1))$ . Consequently, and following [Aitchison and Ho \(1989\)](#), the

correlation function is given by:

$$\rho_Y(\mathbf{h}, \mu, \sigma^2) = \frac{e^{\sigma^2 \rho(\mathbf{h})} - 1}{e^{\sigma^2} - 1 + \mathbb{E}(Y(\mathbf{s}))^{-1}}.$$

This correlation is discontinuous at the origin and the nugget effect is given by:

$$\frac{\mathbb{E}(Y(\mathbf{s}))^{-1}}{\mathbb{E}(Y(\mathbf{s}))^{-1} + e^{\sigma^2} - 1} > 0.$$

It is apparent that the marginal mean  $\mathbb{E}(Y(\mathbf{s}))$  has a strong impact on the nugget effect.

Figure 3 (a) depicts the correlation functions  $\rho_Y(\mathbf{h}, 0.5, 0.05)$ ,  $\rho_Y(\mathbf{h}, 2.5, 0.1)$ , and  $\rho_Y(\mathbf{h}, 4.5, 0.2)$ , which correspond to Poisson LG random fields with mean  $\mathbb{E}(Y(\mathbf{s})) = 1.69$ ,  $12.81$ , and,  $99.48$ , respectively. As underlying correlation model we assume  $\rho(\mathbf{h}) = (1 - \|\mathbf{h}\|/0.5)_+^4$ . It can be appreciated that for large mean values, the nugget effect is negligible. However, for small mean values, the nugget effect can be huge, and it is the cause of the “whitening” effect observed in Figure 2 (a).

Figure 3 (b) depicts the correlation function  $\rho_N(\mathbf{h}, \lambda)$  of the proposed Poisson random field using the same means and underlying correlation function of the Poisson LG random field. It can be appreciated that the correlation is well defined at the origin and covers the entire range between 0 and 1, irrespective of the mean values.

Finally, Figure 3 (c) depicts the correlation function of the Poisson GC random field (Han and De Oliveira, 2016)  $C = \{C(\mathbf{s}), \mathbf{s} \in A\}$  defined as  $C(\mathbf{s}) = F_{\mathbf{s}}^{-1}(\Phi(G(\mathbf{s})), \lambda)$ , where  $\Phi(\cdot)$  is the *cdf* of the standard Gaussian distribution and  $F_{\mathbf{s}}^{-1}(\cdot, \lambda)$  is the quantile function of the Poisson distribution and  $G$  is a standard Gaussian random field with correlation  $\rho(\mathbf{h})$ . The correlation function in this case is given by

$$\rho_C(\mathbf{h}, \lambda) = \int_{-\infty}^{\infty} \int_{-\infty}^{\infty} \lambda^{-1} F_{\mathbf{s}_i}^{-1}(\Phi(z_i), \lambda) F_{\mathbf{s}_j}^{-1}(\Phi(z_j), \lambda) \phi_2(z_i, z_j, \rho(\mathbf{h})) dz_i dz_j - \lambda,$$

where  $\phi_2$  is the *pdf* of the bivariate standard Gaussian distribution. It is apparent that the Poisson GC correlation  $\rho_C(\mathbf{h}, \lambda)$  is much stronger than  $\rho_N(\mathbf{h}, \lambda)$ , and it does not seem to be affected by the different mean values.

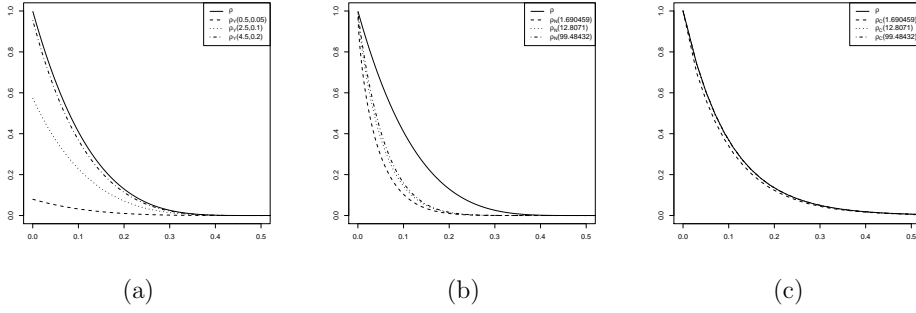


Figure 3: From left to right: (a) correlation functions  $\rho_Y(\mathbf{h}, \mu, \sigma^2)$  of the Poisson LG random field with  $\mu = 0.5, \sigma^2 = 0.05$  and  $\mu = 2.5, \sigma^2 = 0.1$ , and  $\mu = 4.5, \sigma^2 = 0.2$ ; (b) correlation function  $\rho_N(\mathbf{h}, \lambda)$  of our proposed Poisson random field for  $\lambda = 1.69, 12.81$ , and,  $99.48$ ; (c) correlation function  $\rho_C(\mathbf{h}, \lambda)$  of the Poisson GC random field for  $\lambda = 1.69, 12.81$ , and,  $99.48$ . The black line in the Figures depicts the underlying correlation model given by  $\rho(\mathbf{h}) = (1 - \|\mathbf{h}\|/0.5)^4_+$ .

It is important to stress that the proposed Poisson and the Poisson GC random fields that are not mean-square continuous can be obtained by introducing a nugget effect, *i.e.*, a discontinuity at the origin of  $\rho_N(\mathbf{h})$ . This can be achieved by replacing the underlying correlation function  $\rho(\mathbf{h})$  with  $\rho^*(\mathbf{h}) = \rho(\mathbf{h})(1 - \tau^2) + \tau^2 \mathbf{1}_0(\|\mathbf{h}\|)$ , where  $0 \leq \tau^2 < 1$  represents the underlying nugget effect.

### 3.2 Bivariate distribution

In this section, we provide the bivariate distribution of the Poisson random field. This distribution can be written in terms of an infinite series depending on the regularized lower incomplete gamma function defined in (5) and the regularized hypergeometric confluent function (Gradshteyn and Ryzhik, 2007), defined as:

$${}_1\tilde{F}_1(a; b; x) = \frac{{}_1F_1(a; b; x)}{\Gamma(b)} = \sum_{k=0}^{\infty} \frac{(a)_k x^k}{\Gamma(b+k)k!},$$

where  ${}_1F_1$  is the standard hypergeometric confluent function.

For the sake of simplicity, we analyse the following cases separately: (a)  $n = m = 0$ , (b)  $n = 0, m \geq 1$  and  $m = 0, n \geq 1$ , (c)  $n = m = 1, 2, \dots$ , and (d)  $n, m \geq 1, n \neq m$ . Moreover, we set  $p_{nm} = \Pr(N(\mathbf{s}_i) = n, N(\mathbf{s}_j) = m)$ ,  $\lambda_i = \lambda(\mathbf{s}_i)$ ,  $\lambda_j = \lambda(\mathbf{s}_j)$  and  $\rho = \rho(\mathbf{h})$  for notation

convenience. We additionally define the function  $\mathcal{S}$  as follows:

$$\mathcal{S}(a; b; x, x') = {}_1\tilde{F}_1(a; b; x)\gamma^*(c, x').$$

**Theorem 2.** *Let  $N$  be a Poisson random field with underlying correlation  $\rho$  and mean  $\mathbb{E}(N(\mathbf{s}_k)) = \lambda_k$ . Then the bivariate distribution  $p_{nm}$  is given by:*

(a) *Case  $n = m = 0$ :*

$$p_{00} = -1 + e^{-\lambda_i} + e^{-\lambda_j} + (1 - \rho^2) \sum_{k=0}^{\infty} \rho^{2k} \gamma^* \left( k + 1, \frac{\lambda_i}{1 - \rho^2}, \frac{\lambda_j}{1 - \rho^2} \right).$$

(b) *Cases  $n \geq 1, m = 0$  and  $m \geq 1, n = 0$ :*

$$p_{n0} = g(n, \lambda_i, \lambda_j, \rho), \quad p_{0m} = g(m, \lambda_j, \lambda_i, \rho),$$

respectively, where

$$g(b, x, y, \rho) = \frac{x^b}{b!} e^{-x} - x^b e^{-\frac{x}{1-\rho^2}} \sum_{\ell=0}^{\infty} \left( \frac{\rho^2 x}{1 - \rho^2} \right)^\ell \mathcal{S} \left( b; b+\ell+1; \frac{\rho^2 x}{1 - \rho^2}, \frac{y}{1 - \rho^2} \right).$$

(c) *Case  $n = m \geq 1$ :*

$$\begin{aligned} p_{nn} = & - (1 - \rho^2)^n \sum_{k=0}^{\infty} \frac{\rho^{2k} (n)_k}{k!} \gamma^* \left( n + k, \frac{\lambda_i}{1 - \rho^2}, \frac{\lambda_j}{1 - \rho^2} \right) \\ & + \left( \frac{1 - \rho^2}{\rho^2} \right)^n \sum_{k=0}^{\infty} \sum_{\ell=0}^1 \frac{(n)_k}{k!} e^{-\lambda(\mathbf{s}_i)(1-\ell) - \lambda(\mathbf{s}_j)\ell} \gamma^* \left( n + k, \frac{\rho^{2(1-\ell)} \lambda_i}{1 - \rho^2}, \frac{\rho^{2\ell} \lambda_j}{1 - \rho^2} \right) \\ & + (1 - \rho^2)^{n+1} \sum_{k=0}^{\infty} \sum_{\ell=0}^{\infty} \frac{\rho^{2k+2\ell} (n)_\ell}{\ell!} \gamma^* \left( n + \ell + k + 1, \frac{\lambda_i}{1 - \rho^2}, \frac{\lambda_j}{1 - \rho^2} \right). \end{aligned}$$

(d) *Cases  $n \geq 2, m \geq 1$  with  $n > m$ , and  $m \geq 2, n \geq 1$  with  $m > n$ ,*

$$p_{nm} = h(n, m, \lambda_i, \lambda_j, \rho), \quad p_{nm} = h(m, n, \lambda_j, \lambda_i, \rho),$$

respectively, where

$$h(a, b, x, y, \rho) = x^m e^{-\frac{x}{1-\rho^2}} \left[ \sum_{\ell=0}^{\infty} \frac{(b)_{\ell}}{\ell!} \left( \frac{\rho^2 x}{1-\rho^2} \right)^{\ell} \mathcal{S} \left( \begin{matrix} a-b+1 & ; a+\ell+1 \\ & b+\ell \end{matrix}, \frac{\rho^2 x}{1-\rho^2}, \frac{y}{1-\rho^2} \right) - \sum_{k=0}^{\infty} \sum_{\ell=0}^{\infty} \frac{(b)_{\ell}}{\ell!} \left( \frac{\rho^2 x}{1-\rho^2} \right)^{k+\ell} \mathcal{S} \left( \begin{matrix} a-b & ; a+k+\ell+1 \\ & b+k+\ell+1 \end{matrix}, \frac{\rho^2 x}{1-\rho^2}, \frac{y}{1-\rho^2} \right) \right].$$

**Proof.** See the online supplement.

The evaluation of the bivariate distribution can be troublesome at first sight. However, it can be performed truncating the series and taking into account that efficient numerical computation of the regularized lower incomplete gamma and hypergeometric confluent functions can be found in different libraries such as the GNU scientific library (Gough, 2009) and the most important statistical softwares including R, MATLAB and Python. In particular, the R package Geomodels (Bevilacqua et al., 2019) use the Python implementations in the SciPy library (Virtanen et al., 2020).

The bivariate distribution can be written as the product of two independent Poisson distributions when  $\rho_N(\mathbf{h}) = 0$ . This result, provided by Hunter (1974) in Theorem 3.6, establishes that the independence of two renewal counting processes is equivalent to a zero correlation between them. As outlined in Section 3.1,  $\rho(\mathbf{h}) = 0$  implies  $\rho_N(\mathbf{h}) = 0$ . Consequently, pairwise independence at the level of the underlying Gaussian random field implies pairwise independence for the Poisson random field.

We now compare the type of bivariate dependence induced by the proposed model and the GC one when  $\lambda = 5$ . Figure (4) (from left to right) presents the bivariate GC distribution, the bivariate Poisson distribution in Theorem 2 and a coloured image representing the differences between them. Note that a positive value of that difference implies that the probabilities associated with the bivariate distribution in Theorem 2 are greater than the probabilities of the bivariate GC one. Only the probabilities  $\Pr(N(\mathbf{s}_i) = n, N(\mathbf{s}_j) = m)$  for  $n, m = 0, 1, \dots, 12$  are considered in the plots. The first, second and third rows consider increasing levels of underlying correlations  $\rho(\mathbf{h}) = 0.1, 0.5, 0.9$ . The higher the correlation, the more

significant the difference between the bivariate distributions. In addition, if we look at the three coloured Figures as a matrix, a pattern that can be observed is that the probabilities of the proposed bivariate distribution tend to be larger along the main diagonal. This is not surprising since the Poisson GC bivariate distribution inherits the type of dependence of the bivariate Gaussian distribution.

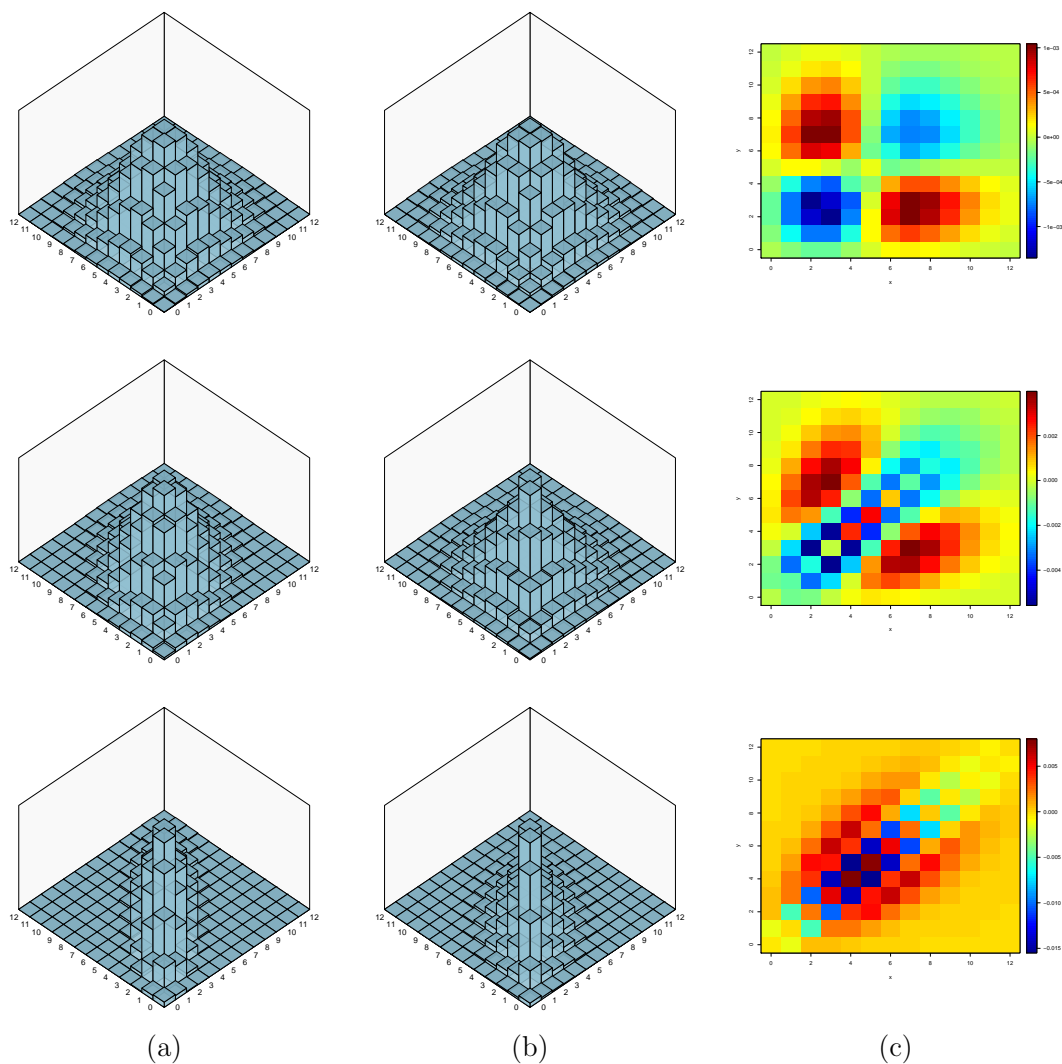


Figure 4: For each row (from left to right): bivariate Poisson GC distribution, our proposed bivariate Poisson distribution and the difference between them. The first, second and third row are obtained setting  $\rho(\mathbf{h}) = 0.1, 0.5, 0.9$  for the underlying correlation.

#### 4. ESTIMATION AND PREDICTION

In this section, we start by describing the weighted pairwise likelihood (*wpl*) estimation method; then, we focus on the optimal linear prediction.

#### 4.1 Weighted pairwise likelihood estimation

Composite likelihood is a general class of objective functions that combine low-dimensional terms based on the likelihood of marginal or conditional events to construct a pseudo likelihood [Lindsay \(1988\)](#); [Varin et al. \(2011\)](#). A particular case of the composite likelihood class is the pairwise likelihood (see for example [Heagerty and Lele, 1998](#); [Bevilacqua and Gaetan, 2015](#); [Alegría et al., 2017](#); [Bevilacqua et al., 2021](#), for application of pairwise likelihood in the spatial setting) that combines the bivariate distributions of all possible distinct pairs of observations. Let  $\mathbf{N} = (n_1, n_2, \dots, n_l)^T$  be a realization of the Poisson random field  $N$  observed at distinct spatial locations  $\mathbf{s}_1, \mathbf{s}_2, \dots, \mathbf{s}_l$ ,  $\mathbf{s}_i \in A$  and let  $\boldsymbol{\theta} = (\boldsymbol{\beta}^T, \boldsymbol{\alpha}^T)$  be the vector of unknown parameters where  $\boldsymbol{\alpha}$  is the vector parameter associated with the underlying correlation model and  $\boldsymbol{\beta}$  the regression parameters. The pairwise likelihood function is defined as follows:

$$\text{pl}(\boldsymbol{\theta}) := \sum_{i=1}^{l-1} \sum_{j=i+1}^l \log(\Pr(N(\mathbf{s}_i) = n_i, N(\mathbf{s}_j) = n_j)) \zeta_{ij},$$

where  $\Pr(N(\mathbf{s}_i) = n_i, N(\mathbf{s}_j) = n_j)$  is the bivariate density given in [Theorem 2](#) and  $\zeta_{ij}$  is a non-negative suitable weight. The choice of cut-off weights, namely,

$$\zeta_{ij} = \begin{cases} 1 & \|\mathbf{s}_i - \mathbf{s}_j\| \leq \xi \\ 0 & \text{otherwise} \end{cases}, \quad (7)$$

for a positive value of  $\xi$ , can be motivated by its simplicity and by observing that the dependence between observations that are distant is weak ([Joe and Lee, 2009](#); [Bevilacqua and Gaetan, 2015](#)).

The maximum weighted pairwise likelihood (*wpl*) estimator is given by:

$$\hat{\boldsymbol{\theta}} := \operatorname{argmax}_{\boldsymbol{\theta}} \text{pl}(\boldsymbol{\theta}).$$

Under some mixing conditions of the Poisson random field ([Bevilacqua et al., 2012](#); [Bevilacqua and Gaetan, 2015](#)), it can be shown that, in the case of increasing domain asymptotic,  $\hat{\boldsymbol{\theta}}$  is consistent and asymptotically Gaussian distributed, with the covariance matrix given by  $\mathcal{G}_n^{-1}(\boldsymbol{\theta})$ , *i.e.*, the inverse of the Godambe information  $\mathcal{G}_n(\boldsymbol{\theta}) := \mathcal{H}_n(\boldsymbol{\theta}) \mathcal{J}_n(\boldsymbol{\theta})^{-1} \mathcal{H}_n(\boldsymbol{\theta})$ , where  $\mathcal{H}_n(\boldsymbol{\theta}) := \mathbb{E}[-\nabla^2 \text{pl}(\boldsymbol{\theta})]$  and  $\mathcal{J}_n(\boldsymbol{\theta}) := \text{Var}[\nabla \text{pl}(\boldsymbol{\theta})]$ . The standard error estimation can be

obtained from the square root diagonal elements of  $\mathcal{G}_n^{-1}(\hat{\boldsymbol{\theta}})$ .

It is important to stress that the computation of the standard errors requires the evaluation of the matrices  $\mathcal{H}_n(\hat{\boldsymbol{\theta}})$  and  $\mathcal{J}_n(\hat{\boldsymbol{\theta}})$ . However, the evaluation of  $\mathcal{J}_n(\hat{\boldsymbol{\theta}})$  is computationally unfeasible for large datasets, and in this case, subsampling techniques can be used, as in [Heagerty and Lele \(1998\)](#) and [Bevilacqua et al. \(2012\)](#). A straightforward and more robust alternative is the parametric bootstrap estimation of  $\mathcal{G}_n^{-1}(\boldsymbol{\theta})$  ([Bai et al., 2014](#)).

Another critical issue related to large datasets is that the computation of the *wpl* estimator can be computationally demanding due to the computational complexity associated with the bivariate Poisson distribution given in [Theorem 2](#). An estimator that requires a smaller computational burden can be obtained by considering a misspecified *wpl* ([Masuda, 2013](#); [Gouriéroux et al., 2017](#); [Bevilacqua et al., 2021](#)). Specifically, suppose that in the estimation procedure, we assume a non-stationary Gaussian random field with mean and variance equal to  $\lambda(\mathbf{s})$  and correlation  $\rho_N(\mathbf{s}_i, \mathbf{s}_j)$  given in [Theorem 1](#). In that case, a (misspecified) Gaussian *wpl* only requires the computation of the Gaussian bivariate distribution.

Gaussian misspecification is a useful inferential tool when the likelihood computation cannot be calculated for some reason, but the first two moments and the correlation are known. Note that the misspecified Gaussian random field matches the mean, variance, and correlation function of the Poisson random field. Additionally, standard maximum likelihood estimation can be performed under the Gaussian misspecification setting.

## 4.2 Optimal linear prediction

The Poisson random field's optimal predictor concerning the mean squared error criterion requires the knowledge of the finite-dimensional distribution, which is not available for the Poisson random field. As in the estimation step, once again, the Gaussian misspecification allows to build an optimal linear predictor based on the correlation of the Poisson random field given in [Theorem 1](#). Specifically, if the goal is the prediction of  $N$  at  $\mathbf{s}_0$  given the vector of spatial observations  $\mathbf{N}$  observed at  $\mathbf{s}_1, \mathbf{s}_2, \dots, \mathbf{s}_l$ , then the optimal linear Gaussian prediction is given by:

$$\widehat{N(\mathbf{s}_0)} = \lambda(\mathbf{s}_0) + \mathbf{c}^T \boldsymbol{\Sigma}^{-1}(\mathbf{N} - \boldsymbol{\lambda}), \quad (8)$$

where  $\boldsymbol{\lambda} = (\lambda(\mathbf{s}_1), \dots, \lambda(\mathbf{s}_l))^T$ ,  $\mathbf{c} = [\sqrt{\lambda(\mathbf{s}_0)\lambda(\mathbf{s}_i)}\rho_N(\mathbf{s}_0, \mathbf{s}_i)]_{i=1}^l$  and  $\Sigma = \sqrt{\boldsymbol{\lambda}\boldsymbol{\lambda}^T} \odot [\rho_N(\mathbf{s}_i, \mathbf{s}_j)]_{i,j=1}^l$  is the variance-covariance matrix ( $\odot$  the matrix Schur product). In practice, the mean and covariance matrix are not known and must be estimated. The associated mean squared error is:

$$\text{MSE}(\widehat{n(\mathbf{s}_0)}) = \lambda(\mathbf{s}_0) - \mathbf{c}^T \Sigma^{-1} \mathbf{c}.$$

Note that this kind of prediction does not guarantee the positivity and discreteness of the prediction. However, in general, optimal linear prediction can be a useful approximation of the optimal predictor, as was shown, for example, in [De Oliveira \(2006\)](#) and recently in [Bevilacqua et al. \(2020\)](#).

## 5. SIMULATION STUDIES

In this section, we focus on two simulation studies. The first one analyses the performance of the *wpl* method when estimating the Poisson random field under the spatial and spatio-temporal settings. The second one analyses the Poisson optimal linear predictor's performance, comparing our approach with the Poisson GC and Poisson LG models.

### 5.1 Performance of the *wpl* estimation

In this study, we consider 1000 realizations from a stationary spatial Poisson random field observed at  $\mathbf{s}_i \in [0, 1]^2$ ,  $i = 1, \dots, l$ ,  $l = 441$ . Specifically, we considered a regular grid with increments of size 0.05 over the unit square  $[0, 1]^2$ . The grid points were perturbed, adding a uniform random value over  $[-0.015, 0.015]$  to each coordinate. A perturbed grid allows us to obtain more stable estimates since different sets of small distances are available and very close location points are avoided.

For the Poisson random field we, consider  $\lambda(\mathbf{s}) = e^\beta$  with  $\beta = \log(2)$ ,  $\log(5)$ ,  $\log(10)$ ,  $\log(20)$ , and an underlying isotropic correlation model  $\rho(\mathbf{h}) = (1 - \|\mathbf{h}\|/\alpha)_+^4$  with  $\alpha = 0.2$ . As outlined in [Section 3.2](#), the use of a compactly supported correlation function simplifies the computation of the bivariate Poisson distribution proposed in [Theorem 2](#).

We study the performance of the Poisson *wpl*, the misspecified Gaussian *wpl* and the misspecified Gaussian maximum likelihood (ML) estimation methods. In the (misspecified) *wpl* estimation, we consider a cut-off weight function, as in [\(7\)](#), with  $\xi = 0.1$ .

	Poisson <i>wpl</i>		Gaussian <i>wpl</i>		Gaussian ML	
	Bias	MSE	Bias	MSE	Bias	MSE
$\beta = \log(2)$	-0.00251	0.00151	-0.00348	0.00161	-0.00366	0.00165
$\alpha = 0.2$	-0.00663	0.00113	-0.00828	0.00208	-0.00748	0.00203
$\beta = \log(5)$	-0.00113	0.00065	-0.00147	0.00068	-0.00161	0.00068
$\alpha = 0.2$	-0.00435	0.00098	-0.00422	0.00149	-0.00344	0.00145
$\beta = \log(10)$	0.00052	0.00033	0.00031	0.00033	0.00014	0.00033
$\alpha = 0.2$	-0.00261	0.00096	-0.00336	0.00120	-0.00296	0.00115
$\beta = \log(20)$	-0.00026	0.00018	-0.00039	0.00019	-0.00037	0.00018
$\alpha = 0.2$	-0.00449	0.00094	-0.00499	0.00099	-0.00402	0.00095

Table 1: Bias and MSE associated with Poisson *wpl*, misspecified Gaussian *wpl* and misspecified Gaussian ML when the true random field is Poisson with  $\lambda(\mathbf{s}) = e^\beta$  and  $\rho(\mathbf{h}) = (1 - \|\mathbf{h}\|/\alpha)_+^4$ .

Table 1 shows the bias and mean squared error associated with  $\beta$  and  $\alpha$  through the four scenarios and three estimation methods. As expected, the misspecified Gaussian ML performs slightly better than the misspecified Gaussian *wpl*. More importantly, it can be recognized that the Poisson *wpl* shows the best performance, particularly when estimating the spatial dependence parameter. This fact is more evident for low counts *i.e.*, when  $\beta$  is decreasing. However, when increasing the mean, the performances of the three methods of estimation tend to be considerably similar, in particular when the mean of the Poisson random field is 20.

To summarize, the Poisson *wpl* is the best method for estimating the Poisson random field when the mean is small (lower than 20 as a rule of thumb in our experiments). For large counts, the misspecified Gaussian *wpl* or ML methods show approximately the same performance as the Poisson *wpl* method.

We also study the proposed methods' performance when estimating a non-stationary version of the Poisson random field. Under the previous simulation setting we changed the constant mean by considering a regression model, that is,  $\lambda(\mathbf{s}) = \exp\{\beta + \beta_1 u_1(\mathbf{s}) + \beta_2 u_2(\mathbf{s})\}$  with  $\beta = 1.5$ ,  $\beta_1 = -0.2$  and  $\beta_2 = 0.3$ , where  $u_1(\mathbf{s})$  and  $u_2(\mathbf{s})$  are independent realizations from a  $(0, 1)$  uniform random variable. Table 2 shows the bias and MSE associated with  $\beta$ ,  $\beta_1$ ,  $\beta_2$  and  $\alpha$  for the three methods of estimation, and Figure 1 of the online supplement plots the associated centred boxplots.

Additionally, in this case, the Poisson *wpl* method shows the best performance. We replicate the simulation by considering larger values of the regression parameters (the results

are not reported here), which lead to larger counts, and the three methods of estimations show approximately the same performance as in the stationary case.

	Poisson <i>wpl</i>		Gaussian <i>wpl</i>		Gaussian ML	
	Bias	MSE	Bias	MSE	Bias	MSE
$\beta = 1.5$	-0.00263	0.00419	-0.00359	0.00445	-0.00320	0.00428
$\beta_1 = -0.2$	0.00189	0.00618	0.00148	0.00665	0.00046	0.00627
$\beta_2 = 0.3$	0.00185	0.00608	0.00202	0.00661	0.00182	0.00621
$\alpha = 0.2$	-0.00148	0.00091	-0.00030	0.00124	0.00096	0.00122

Table 2: Bias and MSE associated with the Poisson *wpl*, misspecified Gaussian *wpl* and misspecified Gaussian ML when estimating a non-stationary Poisson random field with  $\lambda(\mathbf{s}) = \exp\{\beta + \beta_1 u_1(\mathbf{s}) + \beta_2 u_2(\mathbf{s})\}$  and  $\rho(\mathbf{h}) = (1 - \|\mathbf{h}\|/\alpha)_+^4$ .

Finally, we consider a simulation scheme under a spatio-temporal setting. Specifically, we consider 1000 simulations from a non-stationary space-time Poisson random field observed at  $\mathbf{s}_i \in [0, 1]^2$ ,  $i = 1, \dots, l$ ,  $l = 40$  spatial location sites, uniformly distributed within the unit square and  $t_1^* = 0, t_2^* = 0.25, \dots, t_{25}^* = 6$ , 25 time points. We consider a regression model for the spatio-temporal mean  $\lambda(\mathbf{s}, t^*) = \exp\{\beta + \beta_1 u_1(\mathbf{s}, t^*) + \beta_2 u_2(\mathbf{s}, t^*)\}$ , where  $u_k(\mathbf{s}, t^*)$ ,  $k = 1, 2$  are independent realizations from a  $(0, 1)$  uniform random variable. We set  $\beta = 1.5$ ,  $\beta_1 = -0.2$  and  $\beta_2 = 0.3$  as in the previous simulation scheme.

Additionally, as the underlying space-time correlation, we use a simple isotropic and temporal symmetric space-time Wendland separable model  $\rho(\mathbf{h}, t^*) = (1 - \|\mathbf{h}\|/\alpha_s)_+^4 (1 - |t^*|/\alpha_{t^*})_+^4$  with  $\alpha_s = 0.2$  and  $\alpha_{t^*} = 1$ , where  $t^* = t_i^* - t_j^*$  with  $i, j \in \{1, 2, \dots, 25\}$ . Finally, for the misspecified *wpl* estimation, we consider a cut-off weight function as in (7) extended to the space time case, with  $\xi_s = 0.2$  and  $\xi_{t^*} = 0.5$ .

The results concerning this simulation study are shown in Table 3, including the bias and MSE associated with  $\beta$ ,  $\beta_1$ ,  $\beta_2$  and  $\alpha_s$ ,  $\alpha_{t^*}$  for the three estimation methods. In addition, Figure 2 of the online supplement shows the associated box plots. As it can be observed, the Poisson *wpl* approach outperforms the misspecified Gaussian *wpl* and ML as expected for each parameter.

We want to highlight that we have replicated this simulation study by considering higher regression parameters' values, leading to larger counts (for space reasons, these results are not reported here). In that case, all of the estimation methods showed similar behaviours as in the purely spatial case.

	Poisson <i>wpl</i>		Gaussian <i>wpl</i>		Gaussian ML	
	Bias	MSE	Bias	MSE	Bias	MSE
$\beta = 1.5$	-0.00058	0.00166	-0.00120	0.00180	-0.00110	0.00167
$\beta_1 = -0.2$	-0.00079	0.00257	-0.00056	0.00274	-0.00102	0.00249
$\beta_2 = 0.3$	0.00036	0.00284	0.00070	0.00302	0.00062	0.00267
$\alpha_{\mathbf{s}} = 0.2$	-0.01057	0.00464	-0.01323	0.00630	-0.01343	0.00629
$\alpha_{t^*} = 1$	-0.00124	0.01846	0.00165	0.02534	0.00032	0.02415

Table 3: Bias and MSE associated with the Poisson *wpl*, misspecified Gaussian *wpl* and misspecified Gaussian ML when estimating a non-stationary spatiotemporal Poisson random field with  $\lambda(\mathbf{s}, t^*) = \exp\{\beta + \beta_1 u_1(\mathbf{s}, t^*) + \beta_2 u_2(\mathbf{s}, t^*)\}$  and  $\rho(\mathbf{h}, t^*) = (1 - \|\mathbf{h}\|/\alpha_{\mathbf{s}})_+^4 (1 - |t^*|/\alpha_{t^*})_+^4$ .

## 5.2 Performance of the optimal linear prediction

In this section, we compare the performance of the optimal linear predictor of the proposed Poisson random field with the optimal predictors based on the Poisson GC and Poisson LG approaches. To compare the prediction performance of the three approaches, we consider the following steps:

1. Set  $j = 1$ . Repeat until  $j \leq 100$ .
2. Simulate the  $j$ -th spatial dataset from the proposed Poisson random field by considering 300 location sites uniformly distributed on the unit square.
3. Set  $k = 1$ . Repeat until  $k \leq 50$ .
4. Randomly split the  $j$ -th dataset by using 80% of the data for estimation and 20% as the validation dataset.
5. Estimate using *wpl* under our model and using maximum likelihood for the Poisson *GC* and Poisson *LG* models.
6. Compute the optimal linear predictor (8) and the optimal predictor for the Poisson *GC* and Poisson *LG* models at the coordinates associated with the validation dataset, given the estimates obtained at the previous step.
7. Compute, for each model,  $\text{RMSE}_k$ .
8.  $k = k + 1$ . Compute, for each model  $\overline{\text{RMSE}}_j = \sum_{k=1}^{50} \text{RMSE}_k$ .

9.  $j = j + 1$ . Compute, for each model  $\text{RMSE} = \sum_{j=1}^{100} \overline{\text{RMSE}}_j$ .

This numerical experiment has been replicated by simulating (at step 2) from a Poisson GC random field. The simulation settings have been chosen such that the means (and variances) are the same for both models. Specifically, we consider three scenarios with increasing mean, that is 1.69 (scenario 1), 12.81 (scenario 2) and 99.48 (scenario 3). This election generates a Poisson marginal distribution with low, medium and large counts, respectively. Additionally, as the underlying correlation model, we consider  $\rho(\mathbf{h}) = e^{-3\|\mathbf{h}\|/\alpha}$ , with  $\alpha = 0.15$  for the Poisson GC model and  $\alpha = 0.35$  for the Poisson model. This specific setting allows us to obtain similar correlations in both cases.

For the *wpl* estimation of our Poisson model, we set  $\xi = 0.05$  in (7). For the Poisson GC and Poisson LG, we use the maximum likelihood estimation method implemented in the R (R Core Team, 2020) packages `gcKrig` (Han and Oliveira, 2018) and `spaMM` (Rousset and Ferdy, 2014). The `gcKrig` package implements a variant of the sequential importance sampling algorithm and it is used to approximate the Poisson GC likelihood (see Masarotto and Varin, 2017; Han and Oliveira, 2018, for the computational details). The Poisson LG maximum likelihood estimation is computed using Laplace approximations through the `spaMM` package (Rousset and Ferdy, 2014). Finally, the Poisson GC model's optimal prediction, which involves the evaluation of an  $n$ -dimensional integral, is approximated using a variant of the sequential importance sampling algorithm, as in the estimation step.

Table 4 summarizes the results of our experiment, showing the RMSE for each model under the different scenarios and types of model generation. As expected, the prediction using the Poisson LG is the worst in all scenarios. The performance predictions in terms of RMSE of our Poisson and Poisson GC models are quite similar in all scenarios, with a slight preference for the Poisson GC prediction in some of them. This is not surprising since, under the GC model, the optimal predictor is computed. However, the proposed optimal linear predictor is generally very competitive.

In addition, it is important to note that the computations of the ML estimates and the optimal prediction for the Poisson GC model are computationally very intensive, even for a relatively small dataset. To explain, in the previous example (300 location sites) the time

in seconds (measured using the R function `system.time` in a computer laptop with a 2.4 GHz processor and 8 GB of memory) to estimate, using 80% of the data, and to predict, using 20% of the data, require approximately 2.453 seconds and 10.125 seconds, respectively, for the GC model using the package `gcKrig`. On the other hand, the computations of the *wpl* estimates and of the Poisson optimal linear prediction require 0.685 seconds and 0.125 seconds, respectively, using the package `GeoModels`. As a consequence the proposed methods of estimation and prediction are clearly more scalable.

	Scenario 1		Scenario 2		Scenario 3	
	P	PGC	P	PGC	P	PGC
RMSE <sub>P</sub>	1.101410	1.060940	2.792362	2.806396	7.479191	7.751566
RMSE <sub>PGC</sub>	1.102478	1.048888	2.792176	2.786705	7.474412	7.739166
RMSE <sub>PLG</sub>	1.182258	1.155893	3.087286	3.135605	8.437809	8.720756

Table 4: Empirical mean of RMSE associated with the optimal linear predictor of the proposed Poisson random field (P), the optimal predictor based on the Poisson GC (PGC) and Poisson LG (PLG) approaches when the datasets are simulated from the P and PGC models under three scenarios, namely, Scenario 1 (low counts), Scenario 2 (medium counts) and Scenario 3 (large counts).

## 6. APPLICATION TO THE REINDEER PELLET-GROUP SURVEY IN SWEDEN

As mentioned in the Introduction, the pellet-group survey is a technique that provides a general idea of species distribution over a specific geographic area. To assess the impact of newly established wind farms on reindeer habitat, a reindeer pellet-group survey was conducted on Storliden Mountain in the northern forest area of Sweden (Lee et al., 2016). The dataset, which corresponds to the year 2009, has 357 geo-referenced data  $y(\mathbf{s}_i)$ ,  $i = 1, 2, \dots, 357$  and it consists of pellet-group counts where, a pellet-group is defined as a cluster of 20 or more pellets.

The dataset possess two challenging features. The first one is that 73.67% of the counts are zeros because the animal might move as it defecates, and some plots present zero pellet-group counts (see Figure 5). The second one is that the empirical semi-variogram (see Figure 3 of the online supplement) exhibits both spatial correlation and a nugget effect.

To face this problem, we extend the proposed Poisson random field to a zero-inflated Poisson (ZIP) random field for dealing with excess zeros. Specifically, let  $B = \{B(\mathbf{s}), \mathbf{s} \in A\}$ , a Bernoulli random field such that  $B(\mathbf{s}) = \mathbf{1}_{(-\infty, 0)}(G(\mathbf{s}))$ , where  $G$  is a Gaussian random field

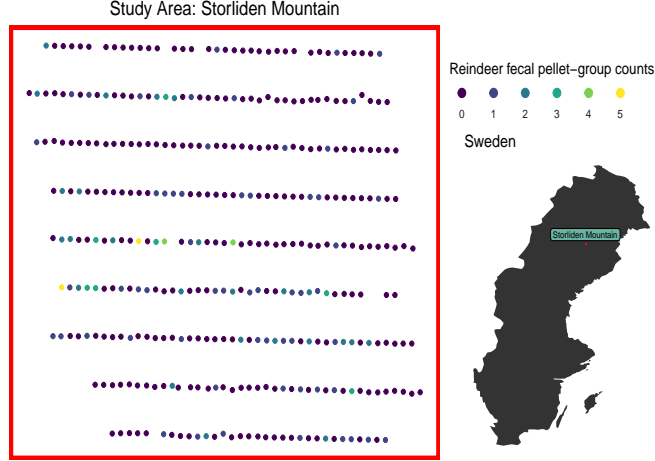


Figure 5: Spatial location of reindeer pellet-group survey data.

with  $\mathbb{E}(G(\mathbf{s})) = \theta(\mathbf{s})$ , unit variance and correlation function  $\rho_1(\mathbf{h})$ . The marginal probability of having a zero is then given by:

$$p(\mathbf{s}) := \Pr(B(\mathbf{s}) = 0) = \Phi(\theta(\mathbf{s})),$$

where  $\Phi$  is the univariate standard Gaussian *cdf*.

Let  $N$  be a Poisson random field with  $\mathbb{E}(N(\mathbf{s})) = \lambda(\mathbf{s})$  and underlying correlation  $\rho_2(\mathbf{h})$ . Assuming  $B$  and  $N$  are independent, the proposed ZIP model is then given by a random field  $Y = \{Y(\mathbf{s}), \mathbf{s} \in A\}$  defined as:

$$Y(\mathbf{s}) := B(\mathbf{s})N(\mathbf{s}), \quad (9)$$

with the marginal distribution given by:

$$\Pr(Y(\mathbf{s}) = y(\mathbf{s})) = \begin{cases} p(\mathbf{s}) + (1 - p(\mathbf{s}))e^{-\lambda(\mathbf{s})} & \text{if } y(\mathbf{s}) = 0 \\ (1 - p(\mathbf{s})) \frac{\lambda(\mathbf{s})^{y(\mathbf{s})} e^{-\lambda(\mathbf{s})}}{y(\mathbf{s})!} & \text{if } y(\mathbf{s}) = 1, 2, \dots \end{cases}, \quad (10)$$

and with  $\mathbb{E}(Y(\mathbf{s})) = (1 - p(\mathbf{s}))\lambda(\mathbf{s})$  and  $\text{Var}(Y(\mathbf{s})) = \mathbb{E}(Y(\mathbf{s}))[1 + \frac{p(\mathbf{s})}{1-p(\mathbf{s})}\mathbb{E}(Y(\mathbf{s}))]$ . Note that the ZIP random field is overdispersed and when  $p(\mathbf{s}) \rightarrow 0$  then the Poisson random field is obtained as special case. For the sake of completeness, we provide the bivariate distribution and the correlation function of the ZIP random field in Proposition 1 (see the online supplement).

For analysing the reindeer pellet-group survey data, we consider the proposed ZIP random

field and we compare it with the ZIP Gaussian copula (ZIP GC) using the R package `gcKrig` (Han and Oliveira, 2018). In addition, we consider the ZIP Log-Gaussian (ZIP LG) random field as implemented in the R package `INLA` (Rue et al., 2009; Lindgren et al., 2011; Martins et al., 2013) which exploits the integrated nested Laplace approximation, under a Bayesian framework, in the estimation step.

Following the results of Lee et al. (2016), we include the following three covariates: Northwest slopes (NS), Elevation (Eln) and Distance to power lines (DPL). In particular we specify  $\lambda(\mathbf{s})$  as:

$$\lambda(\mathbf{s}) = \exp(\beta_0 + \beta_{NS}NS(\mathbf{s}) + \beta_{Eln}Eln(\mathbf{s}) + \beta_{DPL}DPL(\mathbf{s})).$$

The parametrization for the marginal mean and variance are slightly different for the three models. Specifically, assuming a constant probability of excess of zero counts  $p$ , the marginal mean and variance specifications are given by  $\mathbb{E}(Y(\mathbf{s})) = \lambda(\mathbf{s})(1 - p)$  and  $\text{Var}(Y(\mathbf{s})) = \mathbb{E}(Y(\mathbf{s})) \left[ 1 + \frac{p}{1 - p} \mathbb{E}(Y(\mathbf{s})) \right]$  for the proposed model,  $\mathbb{E}(N(\mathbf{s})) = \lambda(\mathbf{s})$  and  $\text{Var}(Y(\mathbf{s})) = \mathbb{E}(Y(\mathbf{s})) [1 + \theta_{GC} \mathbb{E}(Y(\mathbf{s}))]$  for the GC model,  $\mathbb{E}(Y(\mathbf{s})) = \lambda(\mathbf{s}) \exp(0.5\sigma^2)(1 - p)$  and  $\text{Var}(Y(\mathbf{s})) = \mathbb{E}(Y(\mathbf{s})) \left[ 1 + \frac{p}{1 - p} \mathbb{E}(Y(\mathbf{s})) \right] + \mathbb{E}(Y(\mathbf{s}))^2 [\exp(\sigma^2) - 1]$  for the LG model.

Here,  $p$  is specified as  $\Phi(\theta)$ , with  $\theta \in \mathbb{R}$ , as  $\frac{\theta_{GC}}{1 + \theta_{GC}}$ , with  $\theta_{GC} > 0$ , and as  $\frac{\exp(\theta_{LG})}{1 + \exp(\theta_{LG})}$ , with  $\theta_{LG} \in \mathbb{R}$ , respectively, so  $\theta$ ,  $\theta_{GC}$ ,  $\theta_{LG}$  can be interpreted as overdispersion parameters. It is important to remark that  $\beta_0$  can not be compared between the different approaches, but  $\beta_{NS}$ ,  $\beta_{Eln}$  and  $\beta_{DPL}$  can be compared.

We assume an underlying exponential correlation model with nugget effect  $\rho(\mathbf{h}) = (1 - \tau^2)e^{-\|\mathbf{h}\|/\alpha} + \tau^2 \mathbf{1}_0(\|\mathbf{h}\|)$  for the ZIP GC and ZIP LG random fields. On the other hand for the proposed ZIP model we specify  $\rho_1(\mathbf{h}) = (1 - \tau_2^2)e^{-\|\mathbf{h}\|/\alpha} + \tau_2^2 \mathbf{1}_0(\|\mathbf{h}\|)$  and  $\rho_2(\mathbf{h}) = (1 - \tau_1^2)e^{-\|\mathbf{h}\|/\alpha} + \tau_1^2 \mathbf{1}_0(\|\mathbf{h}\|)$  that is two different underlying correlation models for  $B$  and  $N$  in (9) sharing a common exponential correlation model and different nugget effects  $\tau_1^2, \tau_2^2$ .

We use maximum *wpl* estimation with  $\xi = 150$  in (7) for our ZIP random field. For the ZIP GC model we perform maximum likelihood estimation as explained in Section 5.2, and for ZIP LG model, we perform approximate Bayesian inference using the `INLA` approach (Rue et al., 2009).

Table 5 summarizes the results of the estimates, including their standard error for the

three models. In the case of our ZIP random field, standard errors were computed by using parametric bootstrap (Efron and Tibshirani, 1986). For the Poisson LG model the reported estimates are the means of the posterior distributions with associated standard error.

Note that if  $\beta_{DPL}$  is a positive value, then the counts of pellet-groups increase at larger distances from the power lines, *i.e.*, there is a greater reindeer population far from the wind farms. The estimation of the regression parameters are quite similar for our ZIP and the ZIP GC models with lower standard error estimations for the GC model. On the other hand our ZIP model shows the smallest standard error estimation of the spatial scale parameter  $\alpha$ . Finally, the estimates of  $p$ , the excess of zero counts, which depend on  $\theta, \theta_{GC}$  and  $\theta_{LG}$  for the ZIP, ZIP GC and ZIP LG random fields, are given by 0.481, 0.477, 0.573, respectively.

	ZIP	ZIP GC	ZIP LG
$\beta_0$	-23.423890 (6.473000)	-19.096181 (2.308969)	-17.905000 (9.514000)
$\beta_{NS}$	-0.534781 (0.469695)	-0.464979 (0.364517)	-0.826000 (0.388000)
$\beta_{Eln}$	0.005203 (0.004136)	0.003836 (0.002988)	0.010000 (0.005000)
$\beta_{DPL}$	2.594934 (0.742912)	2.060382 (0.265003)	1.622000 (1.177000)
$\theta$	-0.048763 (1.048744)		
$\theta_{GC}$		0.912081 (0.261074)	
$\theta_{LG}$			0.293000 (0.098000)
$\alpha$	339.132404 (92.981918)	298.926862 (186.990640)	685.922925 (354.614010)
$\tau_1^2$	0.868296 (0.263721)		
$\tau_2^2$	0.623987 (0.308045)		
$\tau^2$		0.714227 (0.128536)	0.084655 (0.022749)
$\sigma^2$			0.735290 (0.396332)
RMSE	0.797449	0.801876	0.835611

Table 5: Parameter estimates for the reindeer pellet-group survey data obtained under the ZIP, ZIP GC and ZIP LG random fields. The associated standard errors are in parenthesis. The last row shows the associated empirical mean of the RMSE for each model.

Finally, we want to assess the predictive performances of the three models. To do so, we randomly choose 80% of the spatial locations (*i.e.*, 286 location sites) for the parameter estimation and use the remaining 20% (*i.e.*, 71 location sites) for the predictions. We repeat this procedure a 100 times, recording the RMSE each time. Specifically, for each  $j$ -th left-out

sample  $(y_j(\mathbf{s}_1), y_j(\mathbf{s}_2), \dots, y_j(\mathbf{s}_{71}))$ , we compute

$$\text{RMSE}_j = \left( \frac{1}{71} \sum_{i=1}^{71} (y_j(\mathbf{s}_i) - \hat{Y}_j(\mathbf{s}_i))^2 \right)^{1/2},$$

where  $\hat{Y}_j(\mathbf{s}_i)$  is the optimal linear predictor for our ZIP random field (computed using the correlation given in Proposition 1), the optimal predictor for the ZIP GC random field and the mean of the posterior predictive distribution for the ZIP LG random field. Finally, we report in Table 5, the empirical mean of the RMSE obtained for each left-out sample, *i.e.*,  $\overline{\text{RMSE}} = \sum_{j=1}^{100} \text{RMSE}_j / 100$ . The ZIP and ZIP GC random fields' clearly outperform the ZIP LG random field in terms of prediction performance. In particular the proposed ZIP random field provides the smallest  $\overline{\text{RMSE}}$ .

## 7. CONCLUDING REMARKS

This paper has introduced a model based on a Poisson random field, *i.e.*, a random field with Poisson marginal distributions, for regression and dependence analysis when addressing point-referenced count data defined on a spatial Euclidean space. However, the proposed methodology can be easily adapted to other types of data, such as space-time (Gneiting, 2013), areal (Rue and Held, 2005) or spherical data (Gneiting, 2013).

Our model can be viewed as a spatial generalization of the standard Poisson process since it is obtained by considering sequences of independent copies of a random field with an exponential marginal distribution of inter-arrival times in the counting renewal processes framework. The resulting (non-)stationary random field is marginally Poisson distributed and the dependence is indexed by a correlation function.

The key features of the proposed Poisson random field with respect to the well-known hierarchical Poisson Log-Gaussian random field are that its marginal distribution is Poisson distributed and it can be mean square continuous or not. The Poisson Gaussian copula approach shares these good features with our model. However, the generating mechanisms (*i.e.*, the Poisson process), underlying our model makes it more appealing from interpretability viewpoint.

In our proposal, a possible limitation is that inference based on full likelihood cannot

be performed due to the lack of amenable expressions of the associated multivariate distributions. Nevertheless, the simulations studies we conducted showed that our approach based on a pairwise likelihood estimation seems to be an effective solution for estimating the unknown parameters involved in the Poisson random field. Another potential limitation is that the optimal predictor that minimizes the mean square prediction error is not available. However, our numerical experiments show that our solution based on optimal linear predictor performs very well if compared with the optimal predictors of the Poisson Gaussian copula and Poisson Log Gaussian models.

Finally, the application of our model to the reindeer pellet-group survey data in Sweden shows that our approach can be easily adapted to handle spatial count data with an excessive number of zeros.

A well-known restriction of the Poisson distribution is equidispersion. Unfortunately, this situation is not always observed in real spatial data. The class of random fields proposed in (2) can be used to obtain random fields with flexible marginal models that take into account over or under dispersion. In this case, a possible solution is to consider random fields with a more flexible marginal distribution than the exponential marginal distribution, such as the gamma or Weibull random fields (Bevilacqua et al., 2020). The resulting marginal counting models have been studied in Winkelmann (1995) and McShane et al. (2008). Another alternative for obtaining over dispersed random fields is considering scale mixtures of Poisson random fields. These topics are currently under study and will be included in a forthcoming paper.

#### ACKNOWLEDGEMENTS

The work of Diego Morales-Navarrete, Moreno Bevilacqua and Luis M. Castro was partially supported by ANID - Millennium Science Initiative Program - NCN17\_059 from the Chilean government. Diego Morales-Navarrete also acknowledges support from the VRI-UC scholarship. Moreno Bevilacqua acknowledges FONDECYT grant 1200068, Chile and the regional MATH-AmSud program, grant number 20-MATH-03. The work of Christian Caamaño was partially supported by Proyecto de Iniciación Interno DIUBB 173408 2/I from Universidad del Bío-Bío.

## References

- Aitchison, J. and Ho, C. H. (1989). The multivariate Poisson-Log normal distribution. *Biometrika* **76**, 643–653.
- Alegría, A., Caro, S., Bevilacqua, M., Porcu, E., and Clarke, J. (2017). Estimating covariance functions of multivariate skew-gaussian random fields on the sphere. *Spatial Statistics* **22**, 388 – 402.
- Bai, Y., Kang, J., and Song, P. (2014). Efficient pairwise composite likelihood estimation for spatial-clustered data. *Biometrics* **7**, 661–670.
- Banerjee, S., Carlin, B. P., and Gelfand, A. E. (2014). *Hierarchical Modeling and Analysis for Spatial Data*. Chapman & Hall/CRC Press, Boca Raton: FL.
- Bennett, L., English, P., and McCain, R. (1940). A study of deer populations by use of pellet-group counts. *The Journal of Wildlife Management* **4**, 398–403.
- Bevilacqua, M., Caamaño-Carrillo, C., and Gaetan, C. (2020). On modelling positive continuous data with spatio-temporal dependence. *Environmetrics* **31**, e2632.
- Bevilacqua, M., Caamaño-Carrillo, C., Arellano-Valle, R., and Morales-Oñate, V. (2021). Non-gaussian geostatistical modeling using (skew) t processes. *Scandinavian Journal of Statistics* **48**, 212–245.
- Bevilacqua, M., Faouzi, T., Furrer, R., and Porcu, E. (2019). Estimation and prediction using generalized wendland functions under fixed domain asymptotics. *The Annals of Statistics* **47**, 828–856.
- Bevilacqua, M. and Gaetan, C. (2015). Comparing composite likelihood methods based on pairs for spatial Gaussian random fields. *Statistics and Computing* **25**, 877–892.
- Bevilacqua, M., Gaetan, C., Mateu, J., and Porcu, E. (2012). Estimating space and space-time covariance functions for large data sets: a weighted composite likelihood approach. *Journal of the American Statistical Association* **107**, 268–280.

- Bevilacqua, M., Morales-Oñate, V., and Caamaño-Carrillo, C. (2019). Geomod-els: A package for Geostatistical Gaussian and non Gaussian Data Analysis. <https://vmoprojs.github.io/GeoModels-page/>. R package version 1.0.3-4.
- Buckland, S., Anderson, D. R., Burnham, K. P., Laake, J. L., Borchers, D. L., and Thomas, L. (2001). *Introduction to Distance Sampling-estimating Abundance of Biological Populations*. New York, NY., Oxford University Press.
- Christensen, O. and Waagepetersen (2002). Bayesian prediction of spatial count data using generalized linear mixed models. *Biometrics* **58**, 280–286.
- Cox, D. (1962). *Renewal Theory*. Methuen & Co, London.
- Cressie, N. and Wikle, C. (2011). *Statistics for Spatio-Temporal Data*. Wiley Series in Probability and Statistics. Wiley.
- De Oliveira, V. (2006). On optimal point and block prediction in log-Gaussian random fields. *Scandinavian Journal of Statistics* **33**, 523–540.
- De Oliveira, V. (2013). Hierarchical Poisson models for spatial count data. *Journal of Multivariate Analysis* **122**, 93–408.
- De Oliveira, V. (2014). Poisson kriging: A closer investigation. *Spatial Statistics* **7**, 1–20.
- Diggle, P. and Giorgi, E. (2019). *Model-based Geostatistics for Global Public Health: Methods and Applications*. Chapman & Hall/CRC Interdisciplinary Statistics. Chapman and Hall/CRC Press.
- Diggle, P., Tawn, J., and Moyeed, R. (1998). Model-based geostatistics. *Journal of the Royal Statistical Society: Series C (Applied Statistics)* **47**, 299–350.
- Diggle, P. J. and Ribeiro, P. J. (2007). *Model-based Geostatistics*. Springer, New York.
- Efron, B. and Tibshirani, R. (1986). Bootstrap methods for standard errors, confidence intervals, and other measures of statistical accuracy. *Statistical Science* **1**, 54–75.

- Etten, R. V. and Bennett, C. (1965). Some sources of error in using pellet-group counts for censusing deer. *The Journal of Wildlife Management* **29**, 723–729.
- Gelfand, A. E. and Schliep, E. M. (2016). Spatial statistics and Gaussian processes: A beautiful marriage. *Spatial Statistics* **18**, 86–104. Spatial Statistics Avignon: Emerging Patterns.
- Genest, C. and Nešlehová, J. (2007). A primer of copulas for count data. *ASTIN Bulletin* **37**, 475–515.
- Gneiting, T. (2002). Stationary covariance functions for space-time data. *Journal of the American Statistical Association* **97**, 590–600.
- Gneiting, T. (2013). Strictly and non-strictly positive definite functions on spheres. *Bernoulli* **19**, 1327–1349.
- Gough, B. (2009). *GNU scientific library reference manual*. Network Theory Ltd.
- Gouriéroux, C., Monfort, A., and Renault, E. (2017). Consistent pseudo-maximum likelihood estimators. *Annals of Economics and Statistics* pages 187–218.
- Gradshteyn, I. and Ryzhik, I. (2007). *Table of Integrals, Series, and Products*. Academic Press, New York, 7 edition.
- Guillot, G., Loren, N., and Rudemo, M. (2009). Spatial prediction of weed intensities from exact count data and image-based estimates. *Journal of the Royal Statistical Society: Series C* **58**, 525–542.
- Han, Z. and De Oliveira, V. (2016). On the correlation structure of Gaussian copula models for geostatistical count data. *Australian & New Zealand Journal of Statistics* **58**, 47–69.
- Han, Z. and Oliveira, V. D. (2018). gckrig: An R package for the analysis of geostatistical count data using Gaussian copulas. *Journal of Statistical Software* **87**, 1–32.
- Heagerty, P. and Lele, S. (1998). A composite likelihood approach to binary spatial data. *Journal of the American Statistical Association* **93**, 1099–1111.

- Hunter, J. (1974). Renewal theory in two dimensions: basic results. *Advances in Applied Probability* **6**, 376–391.
- Joe, H. (2014). *Dependence Modeling with Copulas*. Chapman and Hall/CRC, Boca Raton, FL.
- Joe, H. and Lee, Y. (2009). On weighting of bivariate margins in pairwise likelihood. *Journal of Multivariate Analysis* **100**, 670–685.
- Kazianka, H. and Pilz, J. (2010). Copula-based geostatistical modeling of continuous and discrete data including covariates. *Stochastic Environmental Research and Risk Assessment* **24**, 661–673.
- Kibble, W. F. (1941). A two-variate gamma type distribution. *Sankhyā: The Indian Journal of Statistics* **5**, 137–150.
- Krebs, C., Boonstra, R., Nams, V., M, M. O., Hodges, K., and Boutin, S. (2001). Estimating snowshoe hare population density from pellet plots: A further evaluation. *Canadian Journal of Zoology* **79**, 1–4.
- Krishnaiah, P. and Rao, M. (1961). Remarks on a multivariate gamma distribution. *The American Mathematical Monthly* **68(4)**, 342–346.
- Krishnamoorthy, A. S. and Parthasarathy, M. (1951). A Multivariate Gamma-Type Distribution. *The Annals of Mathematical Statistics* **22(4)**, 549–557.
- Lee, Y., Moudud, A., Noh, M., Rönnegård, L., and Skarin, A. (2016). Spatial modeling of data with excessive zeros applied to reindeer pellet-group counts. *Ecology and Evolution* **6**, 7047–7056.
- Lindgren, F., Rue, H., , and Lindstrom, J. (2011). An explicit link between Gaussian fields and Gaussian Markov random fields: the stochastic partial differential equation approach. *Journal of the Royal Statistical Society B* **73**, 423–498.
- Lindsay, B. (1988). Composite likelihood methods. *Contemporary Mathematics* **80**, 221–239.

- Mainardi, F., Gorenflo, R., and Vivoli, A. (2007). Beyond the Poisson renewal process: A tutorial survey. *Journal of Computational and Applied Mathematics* **205**, 725 – 735. Special issue on evolutionary problems.
- Martins, T. G., Simpson, D., Lindgren, F., and Rue, H. (2013). Bayesian computing with inla: new features. *Computational Statistics and Data Analysis* **67**, 68–83.
- Masarotto, G. and Varin, C. (2012). Gaussian copula marginal regression. *Electronic Journal of Statistics* **6**, 1517–1549.
- Masarotto, G. and Varin, C. (2017). Gaussian copula regression in R. *Journal of Statistical Software, Articles* **77**, 1–26.
- Masuda, H. (2013). Convergence of Gaussian quasi-likelihood random fields for ergodic Lévy driven SDE observed at high frequency. *The Annals of Statistics* **41**, 1593–1641.
- Mayle, B., Peace, A., and Gill, R. (1999). How many deer? a field guide to estimating deer population size. Technical Report Forestry Commission Field book 18, Forestry Commission, Edinburgh.
- McShane, B., Adrian, M., Bradlow, E. T., and Fader, P. S. (2008). Count models based on weibull interarrival times. *Journal of Business & Economic Statistics* **26**, 369–378.
- Monestiez, P., Dubroca, L., Bonnin, E., and Guinet, J.-P. D. C. (2006). Geostatistical modelling of spatial distribution of balaenoptera physalus in the northwestern mediterranean sea from sparse count data and heterogeneous. *Ecological Modelling* **193**, 615–628.
- Porcu, E., Bevilacqua, M., and Genton, M. G. (2016). Spatio-temporal covariance and cross-covariance functions of the great circle distance on a sphere. *Journal of the American Statistical Association* **111**, 888–898.
- R Core Team (2020). *R: A Language and Environment for Statistical Computing*. R Foundation for Statistical Computing, Vienna, Austria.
- Ross, S. (2008). *Stochastic Processes, 2nd. Ed.* Wiley series in probability and mathematical statistics. Wiley India Pvt. Limited.

- Rousset, F. and Ferdy, J.-B. (2014). Testing environmental and genetic effects in the presence of spatial autocorrelation. *Ecography* **37**, 781–790.
- Royen, T. (2004). Multivariate Gamma distributions II. In *Encyclopedia of Statistical Sciences*, pages 419–425. New York: John Wiley & Sons.
- Rue, H. and Held, L. (2005). *Gaussian Markov Random Fields: Theory and Applications*. Chapman & Hall, London.
- Rue, H., Martino, S., and Chopin, N. (2009). Approximate Bayesian inference for latent Gaussian models using integrated nested Laplace approximations (with discussion). *Journal of the Royal Statistical Society B* **71**, 319–392.
- Sivertsen, T. R., Åhman, B., Steyaert, S. M. J. G., Rönnegård, L., Frank, J., Segerström, P., Støen, O.-G., and Skarin, A. (2016). Reindeer habitat selection under the risk of brown bear predation during calving season. *Ecosphere* **7**, e01583.
- Stein, M. (1999). *Interpolation of Spatial Data. Some Theory of Kriging*. Springer-Verlag, New York.
- Trivedi, P. and Zimmer, D. (2017). A note on identification of bivariate copulas for discrete count data. *Econometrics* **5(1)**, 1–11.
- Varin, C., Reid, N., and Firth, D. (2011). An overview of composite likelihood methods. *Statistica Sinica* **21**, 5–42.
- Vere-Jones, D. (1997). Alpha-permanents and their applications to multivariate gamma, negative binomial and ordinary binomial distributions. *New Zealand Journal of Mathematics* **26**, 125–149.
- Virtanen, P., Gommers, R., Oliphant, T., Haberland, M., Reddy, T., Cournapeau, D., Burovski, E., Peterson, P., Weckesser, W., Jonathan, B., van der Walt, J., S., Brett, M., Wilson, J., Jarrod Millman, K., Mayorov, N., and et al. (2020). SciPy 1.0: Fundamental Algorithms for Scientific Computing in Python. *Nature Methods* **17**, 261–272.

Winkelmann, R. (1995). Duration dependence and dispersion in count-data models. *Journal of Business & Economic Statistics* **13**, 467–474.